Structure and magnetization of arrays of electrodeposited Co wires in anodic alumina

Please check the document version of this publication:

• A submitted manuscript is the version of the article upon submission and before peer-review. There can be important differences between the submitted version and the official published version of record. People interested in the research are advised to contact the author for the final version of the publication, or visit the DOI to the publisher's website.
• The final author version and the galley proof are versions of the publication after peer review.
• The final published version features the final layout of the paper including the volume, issue and page numbers.

[Link to publication](#)

Structure and magnetization of arrays of electrodeposited Co wires in anodic alumina

G. J. Strijkers,[a] J. H. J. Dalderop, M. A. A. Broeksteeg, H. J. M. Swagten, and W. J. M. de Jonge

Department of Physics and Research School COBRA, Eindhoven University of Technology, P. O. Box 513, 5600 MB Eindhoven, The Netherlands

We have produced arrays of Co nanowires in anodic porous alumina filters by means of electrodeposition. The structure and magnetization behavior of the wires was investigated with nuclear magnetic resonance (NMR) and magnetization measurements. NMR shows that the wires consist of a mixture of fcc and hcp texture with the (0001) texture of the hcp fraction oriented preferentially perpendicular to the wires. The magnetization direction is determined by a competition of demagnetizing fields and dipole–dipole fields and can be tuned parallel or perpendicular to the wires by changing the length of the wires. © *1999 American Institute of Physics.* [S0021-8979(99)00421-1]

I. INTRODUCTION

The fabrication and properties of arrays of tunable magnetic nanostructures are of interest not only from a fundamental, but also from a technological point of view, as recording technologies in the future will require higher bit densities to fulfill the unrelenting demand for more storage capacities. There are several approaches to fabricate large arrays of magnetic structures, for example, by lithographic techniques such as electron beam lithography and ion beam lithography. The disadvantage of these techniques is that they are expensive and it is time consuming to write nanostructures on large scales, although recently[1] optical interference techniques are being developed to circumvent this problem. Another way to fabricate large scale periodic nanostructures is by electrodeposition of magnetic materials in the pores of nuclear track etched polycarbonate membranes[2–6] or in the pores of self-ordered nanochannel material formed by anodization of Al in an acid solution,[7–10] a low cost and fast technique to produce large arrays of identical magnetic entities, with a very large aspect ratio (length divided by diameter), which is not possible with standard lithographic techniques. Wires in anodic alumina have the advantage above wires in polycarbonate membranes in that they are completely parallel and exactly perpendicular to the membrane surface and, moreover, the wires are assumed to have a constant diameter[11] throughout their entire length.

Specifically, here we present a study of the structure and magnetization behavior of Co wires electrodeposited in commercially[12] available nanoporous alumina, with nominal pore diameters of 100 and 20 nm. Nuclear magnetic resonance (NMR) is used to determine the microstructure of the wires and it will be shown that the crystallographic structure of the Co wires consists of a mixture of fcc and hcp stacking.

The crystallographic quality of the Co is comparable to sputtered or molecular beam epitaxy (MBE) grown Co layers. The magnetization behavior, studied with direct magnetization measurements and through the anisotropy of the resonance fields, is determined by a competition of self-demagnetization of the wires and dipolar interactions between the wires. It will be shown that dipolar interactions can lead to a preferential direction of the magnetization perpendicular to the wires, which can be tuned by changing the length of the wires.

II. EXPERIMENT

As a starting material, commercially available[12] nanoporous alumina filters were used with a thickness of 60 μm and nominal pore diameters of 100 and 20 nm. Scanning electron microscopy (SEM) images of the surface of the filters suggest that the diameter of the pores is up to a factor of 2 larger than the nominal diameter. However, we will refer in the rest of this article to the nominal pore diameter as the precise diameter of the pores is not crucial for our analysis. The nominal pore density is $1 \times 10^{13}/m^2$ in both cases, which is confirmed by SEM images, yielding an average spacing between individual pores of approximately 320 nm. One side of the filters was covered with a few μm-thick-dc-sputtered gold layer to obtain a conducting base layer at the bottom of the pores. The Co wires were then grown by electrodeposition of Co^{2+} ions from an electrolyte with the following composition: 400 g $CoSO_4 \cdot 7H_2O$, 40 g H_3BO_3, and 1 ℓH_2O. Deposition is performed in an ertalyte cell with the nanopores facing upwards at a deposition potential of $U_{Co} = -1.05$ V with respect to a saturated calomel reference electrode (SCE). The total thickness of the alumina filter is 60 μm. Deposition is stopped when the desired wirelength is reached, which was determined from the total integrated charge passing between the working electrode and the counter electrode. The length of the wires was separately

[a]Author to whom correspondence should be addressed. Electronic mail: Strijkers@phys.tue.nl
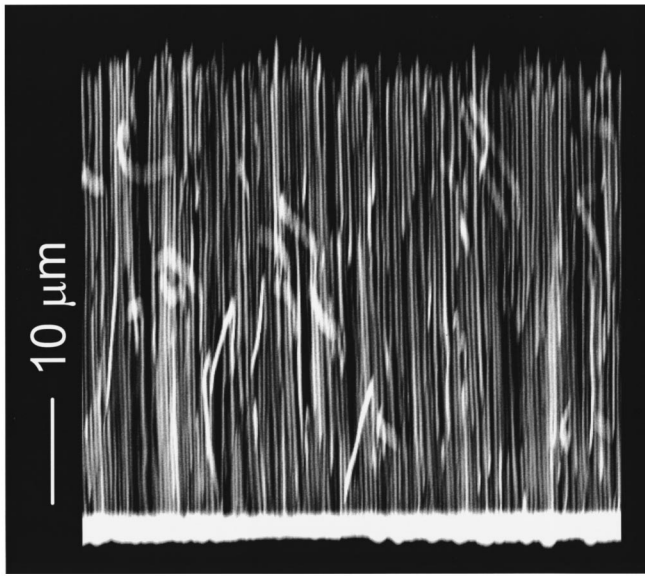
FIG. 1. Cross section SEM picture of Co wires in 20 nm anodic alumina fiber. The bright broad line at the bottom of the figure is the gold base layer.

checked after deposition with cross section SEM images and with a normal light microscope and is found to be uniform within 5%. The area of deposition is approximately 1 cm^2, which can easily be enlarged to fabricate larger arrays of wires. NMR measurements were performed with a phase coherent spin-echo spectrometer at $T = 4.2$ K in the frequency range between 195 and 235 MHz and fields up to 4.5 T. Magnetization measurements were done with a Quantum Design superconducting quantum interference device (SQUID).

In Fig. 1 a cross section SEM image is shown for Co wires grown in 20 nm anodic alumina. The bright broad line at the bottom of the figure is the Au base layer with a thickness of about 3 μm. As can be seen, the individual wires are very straight indeed and parallel with a length of about 40 μm, which corresponds to an aspect ratio of about 2000. To obtain a cross section image the filter was broken which is probably the reason why some of the wires seem somewhat distorted and blurred in the picture. SEM images of the surface show that the array of pores is rather disordered and not hexagonally ordered as they were produced recently.[13]

III. RESULTS AND DISCUSSION

Figure 2 shows zero-field and field-swept NMR spectra of our 100 and 20 nm Co wires. All spectra are recorded at 4.2 K and corrected for enhancement of the spin-echo signal because of oscillations of the electronic moment.[14] We have used NMR because it is a powerful technique[14–16] to probe the microstructure of Co. Furthermore, through the anisotropy of the resonance fields we can obtain valuable information on the magnetic behavior. Figure 2(a) and 2(d) show the zero applied field NMR spectra of the 100 and the 20 nm wires. In both spectra a clear peak can be distinguished at about 217 MHz which corresponds to fcc Co and contributes to about 40% of the total spectrum. To the right of this fcc peak a mixture of hcp Co and stacking faults (twinning, deformation, etc.) are visible. Co in hcp structure gives rise to
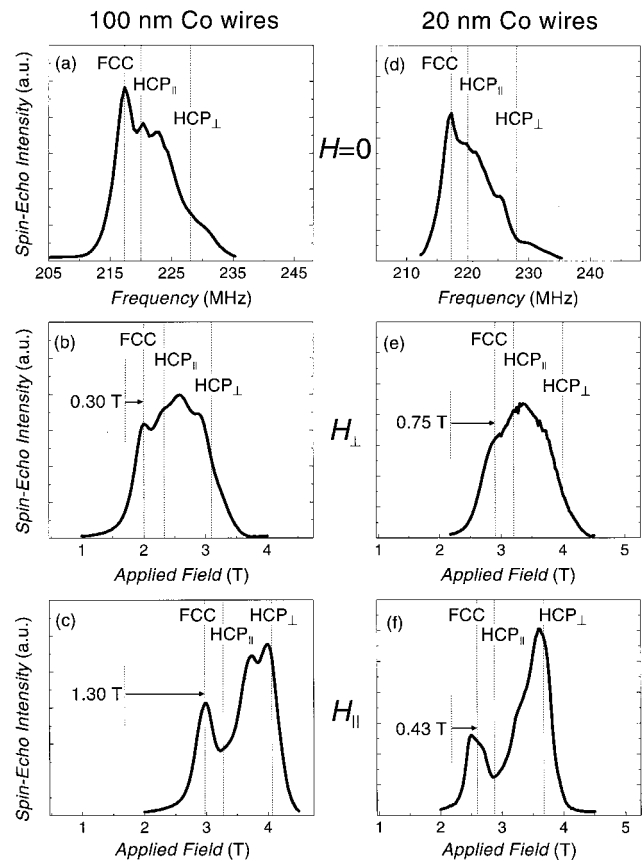

FIG. 2. ^{59}Co nuclear magnetic resonance spectra of 100 and 20 nm wires. (a) and (d) Spin-echo intensity as function of frequency in zero field. (b) and (e) Spin-echo intensity as function of an applied field perpendicular to the wires. (c) and (f) Spin-echo intensity as function of an applied field parallel to the wires. The arrows indicate the shift of the spectra with respect to the zero-field spectra. The line positions of fcc Co and hcp Co are indicated with the dashed lines. Spectra (b) and (c) are recorded at a frequency of 200 MHz; (e) and (f) at 195 MHz.

a resonance frequency along the c axis (hcp$_\parallel$) at 20 MHz and perpendicular to the c axis (hcp$_\perp$) at 228 MHz. On the left hand side of the fcc peak the intensity does not drop to zero completely which might be caused by Co atoms at the interfaces with Al$_2$O$_3$ or by grain boundaries.[16] The zero-field spectra resemble NMR spectra of sputtered[16] and even MBE grown[15] Co layers, which indicates that the crystallographic quality of our Co wires can be compared to layers made with other fabrication techniques.

The resonance condition for NMR in this configuration is

$$f = \frac{\gamma}{2\pi}(B_{hf} - B_{appl} + B_{surr} + B_{dem}) \qquad (1)$$

with B_{surr} the field produced by the surrounding Co lines and B_{dem} the self-demagnetizing field of the wires. In an in-plane magnetized uniform film the last two fields are not present. For long wires, however, B_{dem} perpendicular to the wire axis is $\frac{1}{2}M_s$ (≈ 0.9 T), with M_s the saturation magnetization of Co,[17] and wire–wire interactions can lead to a sizable B_{surr}. From Eq. (1) it is clear that we can measure B_{surr} by recording a NMR spectrum as a function of an externally applied field and hence we can gain more insight into the magnitude

of the wire–wire interactions. In Figs. 2(b), 2(c), 2(e), and 2(f) the NMR spectra at constant frequency of the 100 and 20 nm wires are shown as function of the field applied either perpendicular or parallel to the wires. The horizontal axes of the spectra are plotted in such a way that they scale with the frequency axes of the zero-field spectra via Eq. (1), assuming $B_{surr} + B_{dem} = 0$. This means that the line shifts indicated with arrows in Fig. 2 are equal to $B_{surr} + B_{dem}$. First we consider the spectrum of 100 nm Co wires with the applied field perpendicular to the wires [Fig. 2(b)]. With respect to the zero-field spectrum of Fig. 2(a) the overall spectrum is shifted with about 0.3 T, which gives $B_{surr} = -0.6$ T using $B_{dem} = 0.9$ T. Figure 2(c) shows the NMR spectrum with the applied field along the wire axes. The shift with respect to the zero-field spectrum is about 1.30 T, even higher than with the field perpendicular to the wires, and because $B_{dem} = 0$ along the wire axis this results in $B_{surr} = 1.30$ T. Apparently, for the 100 nm Co wires the surrounding field introduces an easy axis perpendicular to the wires, although a magnetization along the wires axes was expected from the magnitude of the self-demagnetizing field of the long wires. On the other hand, the 20 nm wires behave more isotropic with a small preference for the magnetization parallel to the wires. The overall shift of the spectrum is about 0.75 T when the applied field is perpendicular to the wires and only 0.43 T when the applied field is parallel to the wires, leading to $B_{surr} = -0.15$ T and $B_{surr} = 0.43$ T, respectively.

Before focusing further on this magnetization behavior for the different wire diameters, first the shape of the NMR spectra will be discussed in more detail. The NMR spectra with the field perpendicular to the wire in Figs. 2(b) and 2(e) consist of a fcc Co peak, hcp$_\parallel$ and hcp$_\perp$, and stacking faults, which are also located at the right hand side of the fcc peak.[15] When the field is applied parallel to the wires a dip in the spectra appears at the position of hcp$_\parallel$ and when the field is applied perpendicular to the wires there is less intensity at the position of hcp$_\perp$, from which directly follows that the texture of the hcp Co fraction is mainly with the *c* axis perpendicular to the wires. As a result, an extra anisotropy contribution of the magnetic anisotropy along the *c* axis has to be taken into account. This also was observed in electrodeposited Co wires in polycarbonate membranes by Ounadjela *et al.*[4] and by Piraux *et al.*[18]

Now we will discuss in more detail the magnetization behavior of the wires. Figure 3 shows the magnetization measurements for the 100 and 20 nm Co wires. The saturation fields are qualitatively in agreement with the shift of the NMR spectra indicated with arrows in Fig. 2. The 100 nm Co wires are more easily saturated perpendicular to the wires than parallel to the wire axes, while the 20 nm wires behave more isotropic as saturation is reached at approximately the same value for the field parallel and perpendicular to the wires. From this we conclude that the magnetization behavior is mainly a result of a competition of demagnetization of the individual wires and dipole–dipole interaction between the wires.

The small differences in magnitude between the saturation fields observed in the magnetization measurements and the shifts of the NMR spectra are caused by the magneto-
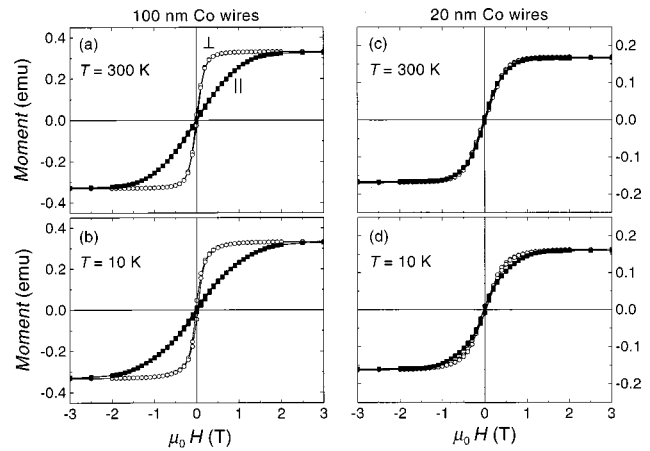

FIG. 3. Magnetization hysteresis curves of 100 nm wires (a) and (b) and 20 nm wires (c) and (d) at 300 and 10 K, with the applied field perpendicular (open circles) and parallel (solid squares) to the wires.

crystalline anisotropy of the hcp Co fraction, which does affect the shape of the magnetization curve in a way that it slightly favors a magnetization direction perpendicular to the wires, but does not add to the shift of the NMR spectra. Therefore, saturation for the 20 nm wires [see Fig. 3(d)] with field parallel to the wires is reached at higher fields than for the field perpendicular to the wires, while the NMR spectra [see Figs. 2(e) and 2(f)] suggest a slight tendency for an easy axis of magnetization parallel to the wires. Because the crystalline anisotropy of hcp Co decreases at higher temperature[19] the saturation fields parallel to the wires decrease at higher temperatures.

From a simple consideration we can understand that a competition of dipole–dipole interactions and demagnetization can lead to a preferential direction of magnetization perpendicular to the wires. The array of wires may be approximated as a two dimensional infinite array of magnetic dipoles located on a square grid. The total field acting on one wire is the total dipole sum produced by all the other wires and reads[20,21]

$$B_z = 4.2 \frac{\mu_0}{4\pi} \cdot \frac{p}{d^3} \qquad (2)$$

when all the moments are aligned along the wires. Here, *p* is the moment of one wire and *d* the distance between the wires. When all the moments are aligned perpendicular to the wires the total field acting on one wire is the sum of the dipole fields and the self-demagnetizing field of the wire

$$B_x = -2.1 \frac{\mu_0}{4\pi} \cdot \frac{p}{d^3} + B_{dem}. \qquad (3)$$

The sign of B_z and B_x is chosen with reference to Eq. (1), that is opposite to the applied field. Depending on the magnitude of the moment *p*, which in our experiments can be chosen by changing the wire length or diameter, either B_z or B_x is smallest leading to an easy direction of magnetization parallel or perpendicular to the wires, respectively.

We realize that this model based on a uniform magnetization reversal is in principle too simple and does not describe detailed magnetization reversal processes in the wires.
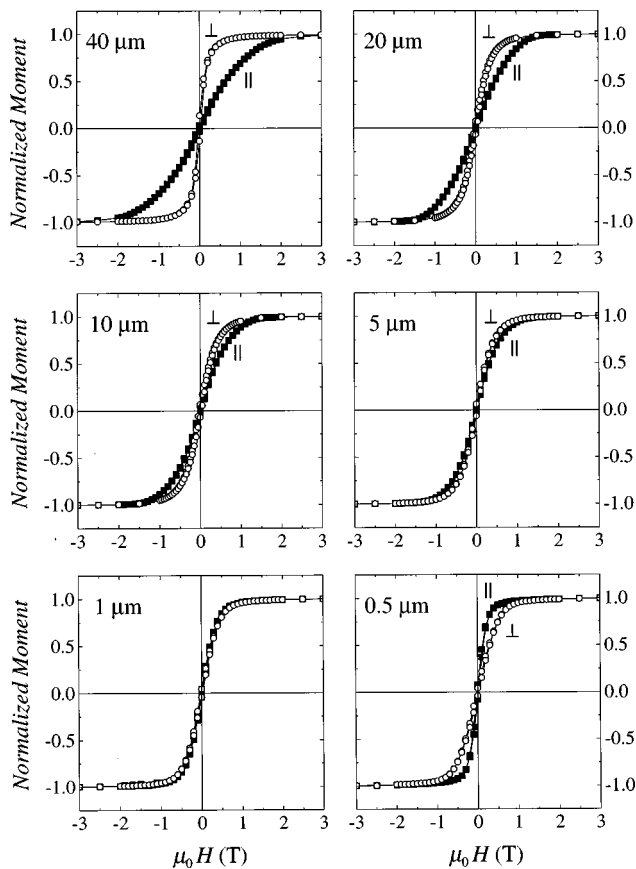
FIG. 4. Magnetization hysteresis curves of 100 nm wires as a function of the wire length at 10 K, with the applied field perpendicular (open circles) and parallel (solid squares) to the wire axes.
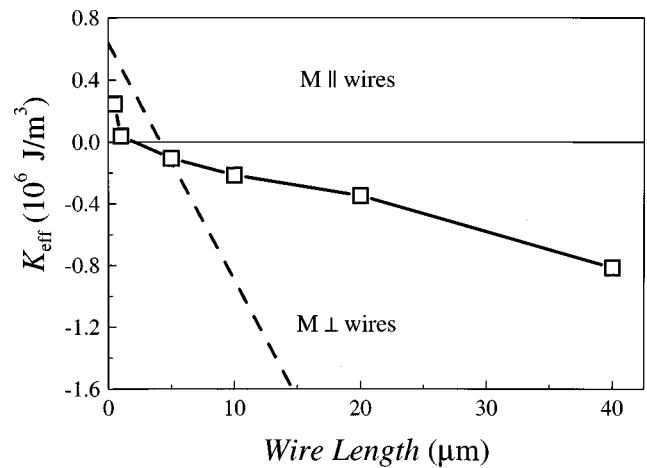

FIG. 5. Effective anisotropy constant K_{eff} as function of wire length; measured (open squares) and calculated (dashed line) from Eqs. (2) and (3).

Including these would require extensive micromagnetical calculations, which are far beyond the scope of this article. Nevertheless, as will be shown in the following, we can qualitatively describe the basic magnetization behavior with our simple magnetostatic model.

In accordance with the previous predictions, we have experimentally observed such a transition, as shown in Fig. 4. When the wire length is decreased from 40 to 0.5 μm a crossover takes place from a perpendicular easy direction of magnetization towards an easy direction parallel to the wires. This can be quantified by the effective anisotropy constant K_{eff}, derived from the magnetic anistropy density, that is the area between the magnetization curves with field orientation parallel and perpendicular to the wire axes, which is presented in Fig. 5. The magnetostatic energy E per unit volume is given by $E = -K_{eff} \times \cos^2 \theta$, with θ the angle between the wire axes and the magnetization direction. A change from easy axis of magnetization perpendicular ($K_{eff} < 0$) to parallel ($K_{eff} > 0$) occurs at a wire length of about 1 μm.

Assuming a diameter of 100 nm and an average distance between the wires of 320 nm we have calculated the effective anisotropy constant as function of the wire length from Eqs. (2) and (3), which also is shown in Fig. 5 (dashed line). The calculated change from perpendicular to parallel magnetization ($K_{eff} = 0$) at about 4 μm is in reasonable agreement with the measured change at 1 μm. Moreover, as mentioned before, we have some indications from SEM images that the

actual diameter of the wires is up to a factor of 2 larger than the nominal diameter, which would explain this difference of a factor of 4. However, the calculated magnitude is much larger than the measured K_{eff}, especially for the longest wires, when clearly the assumption of two dimensional array of magnetic dipoles no longer holds. As already mentioned before, the analysis of K_{eff} is based on a uniform magnetization reversal without domain wall motion, curling or buckling of the magnetization in the wires, which lead to a smaller effective anisotropy than for purely magnetostatic interactions. Furthermore, for the sample with the shortest wires we may have to consider the possibility that, due to inhomogeneities in the electrodeposition process, part of the pores is not filled. This also would lead to a decrease of the dipole interactions and could account for the sharp increase in K_{eff}. Although we cannot rule out these inhomogeneities completely, the NMR linewidths for these short wires are not significantly different from those observed in Fig. 2, as would be the case for inhomogeneities growth with a large spread in dipole fields.

IV. CONCLUSIONS

In summary, we have produced large arrays of identical Co nanowires by electrodeposition in commercially available anodic alumina. We have demonstrated that the magnetization behavior is determined by a competition of demagnetizing fields and dipole–dipole interactions and to a lesser extent by magnetocrystalline anisotropy. The easy direction of magnetization can be tuned either perpendicular or parallel to the wires by changing the length of the wires.

ACKNOWLEDGMENTS

[1] E. F. Wassermann, M. Thielen, S. Kirsch, A. Pollmann, H. Weinforth, and A. Carl, J. Appl. Phys. **83**, 1753 (1998).

[2] L. Piraux, J. M. George, J. F. Despres, C. Leroy, E. Ferain, and R. Legras, Appl. Phys. Lett. **65**, 2484 (1994).

[3] A. Blondel, J. P. Meier, B. Doudin, and J. P. Ansermet, J. Appl. Phys. **65**, 3019 (1994).

[4] K. Ounadjela, R. Ferré, L. Louail, J. M. George, and J. L. Maurice, J. Appl. Phys. **81**, 5455 (1997).

[5] G. P. Heydon, S. R. Hoorn, A. N. Farley, S. L. Tomlinson, M. S. Valera, K. Attenborough, and W. Schwarzacher, J. Phys. D **30**, 1083 (1997).

[6] J. L. Maurice, D. Imhoff, P. Etienne, O. Durand, S. Dubois, L. Piraux, J. M. George, P. Galtier, and A. Fert, J. Magn. Magn. Mater. **184**, 1 (1998).

[7] S. Bandyopadhyay, A. E. Miller, H. C. Chang, G. Banerjee, V. Yuzhakov, D. F. Yue, R. E. Ricker, S. Jones, J. A. Eastman, E. Baugher, and M. Chandrasekhar, Nanotechnology **7**, 360 (1996).

[8] H. Masuda, H. Yamada, M. Satoh, and H. Asoh, Appl. Phys. Lett. **71**, 2770 (1997).

[9] D. N. Davydov, J. Haruyama, D. Routkevitch, B. W. Statt, D. Ellis, M. Moskovits, and J. M. Xu, Phys. Rev. B **57**, 13550 (1998).

[10] W. Schwarzacher, presented at the 3rd International Symposium on Metallic Multilayers (MML'98), Vancouver, Canada, June 14–19, 1998.

[11] C. Schönenberger, B. M. I. van der Zande, L. G. J. Fokkink, M. Henny, C. Schmid, M. Krüger, A. Bachtold, R. Huber, H. Birk, and U. Staufer, J. Phys. Chem. B **101**, 5497 (1997).

[12] The anodic alumina filters were obtained from Whatman International Ltd., Maidstone, England.

[13] O. Jessenksy, F. Müller, and U. Gösele, Appl. Phys. Lett. **72**, 1173 (1998).

[14] P. Panissod, in *Topics in Current Physics*, edited by U. Gonser (Springer, Berlin, 1986), Vol. 40, p. 365.

[15] H. A. M. de Gronckel, P. J. H. Bloemen, E. A. M. van Alphen, and W. J. M. de Jonge, Phys. Rev. B **49**, 11327 (1994).

[16] P. Panissod, J. P. Jay, C. Meny, M. Wojcik, and E. Jedryka, Hyperfine Interact. **97/98**, 75 (1996).

[17] R. I. Joseph and E. Schlömann, J. Appl. Phys. **36**, 1579 (1965).

[18] l. Piraux, S. Dubois, E. Ferain, R. Legras, K. Ounadjela, J. M. George, J. L. Maurice, and A. Fert, J. Magn. Magn. Mater. **165**, 352 (1997).

[19] D. M. Paige, B. Szpunar, and B. K. Tanner, J. Magn. Magn. Mater. **44**, 239 (1984).

[20] J. Jackson, *Classical Electrodynamics* (Wiley, New York, 1962).

[21] M. Grimditch, Y. Jaccard, and I. K. Schuller, Phys. Rev. B **58**, 11539 (1998).